energies

Article

A Multi-Objective Life Cycle Optimization Model of an Integrated Algal Biorefinery toward a Sustainable Circular Bioeconomy Considering Resource Recirculation

Celine Marie A. Solis [1,*], Jayne Lois G. San Juan [1,2], Andres Philip Mayol [3], Charlle L. Sy [1,2], Aristotle T. Ubando [2,3] and Alvin B. Culaba [2,3]

[1] Industrial Engineering Department, De La Salle University, Manila 0922, Philippines; jayne.sanjuan@dlsu.edu.ph (J.L.G.S.J.); charlle.sy@dlsu.edu.ph (C.L.S.)
[2] Center for Engineering and Sustainable Development Research, De La Salle University, Manila 0922, Philippines; aristotle.ubando@dlsu.edu.ph (A.T.U.); alvin.culaba@dlsu.edu.ph (A.B.C.)
[3] Mechanical Engineering Department, De La Salle University, Manila 0922, Philippines; andres_mayol@dlsu.edu.ph
* Correspondence: celine_solis@dlsu.edu.ph

Abstract: Biofuel production from microalgae biomass has been considered a viable alternative to harmful fossil fuels; however, challenges are faced regarding its economic sustainability. Process integration to yield various high-value bioproducts is implemented to raise profitability and sustainability. By incorporating a circular economy outlook, recirculation of resource flows is maximized to yield economic and environmental benefits through waste minimization. However, previous modeling studies have not looked into the opportunity of integrating productivity reduction related to the continuous recirculation and reuse of resources until it reaches its end of life. In this work, a novel multi-objective optimization model is developed centered on an algal biorefinery that simultaneously optimizes cost and environmental impact, adopts the principle of resource recovery and recirculation, and incorporates the life cycle assessment methodology to properly account for the environmental impacts of the system. An algal biorefinery involving end-products such as biodiesel, glycerol, biochar, and fertilizer was used for a case study to validate the optimization model. The generated optimal results are assessed and further analyzed through scenario analysis. It was seen that demand fluctuations and process unit efficiencies have significant effect on the optimal results.

Keywords: algal biofuel; algal biorefinery; life cycle optimization; mixed integer nonlinear programming

Citation: Solis, C.M.A.; San Juan, J.L.G.; Mayol, A.P.; Sy, C.L.; Ubando, A.T.; Culaba, A.B. A Multi-Objective Life Cycle Optimization Model of an Integrated Algal Biorefinery toward a Sustainable Circular Bioeconomy Considering Resource Recirculation. *Energies* **2021**, *14*, 1416. https://doi.org/10.3390/en14051416

Academic Editor: Poul Alberg Østergaard

Received: 26 January 2021
Accepted: 26 February 2021
Published: 4 March 2021

1. Introduction

The overwhelming environmental concerns associated with fossil fuel production and consumption are only expected to rise in the following years as global energy demand grows by around 1.3% every year [1]. This proves that further research into alternative renewable sources of energy is necessary [2]. Biodiesel, which is considered as the main substitute for fossil fuel, has numerous biomass feedstock alternatives, with microalgae being considered the most valuable due to its high growth productivity and photosynthetic efficiency [3–5]. Microalgae are aquatic microorganisms that grow in the process of photosynthesis, converting nutrients (carbon dioxide, water, etc.) into energy [6,7]. In addition, growing microalgae uses a lower area of arable land compared to other biofuel candidates such as corn, soybean, canola, and jatropha [8]. One of the promising attributes that makes microalgae a viable option for alternative biofuel is the ability to harness carbon dioxide from the atmosphere [9].

However, economic limitations are faced when looking into microalgal biofuel production due to its higher overall costs as compared to the production of fossil fuels. Proper investment strategies were found to be an integral factor to ensure long-term sustainability and growth in the diffusion of algal biofuel [10]. Aside from that, the processes involved in biofuel production typically generate a lot of waste including unused biomass waste. To maximize the algal biomass used in biofuel production, integrated process methods are incorporated into the production system through biorefineries. An algal biorefinery is built to produce energy and along with other products derived from biomass. Examples of these are biogas, biodiesel, bioethanol, fertilizers, and cosmetics. The incorporation of additional high-value products leads to increased profitability and biomass utilization for the biorefinery.

With that, numerous researchers have investigated the integration of processes with the aim of a zero-waste biofuel production system. Mitra and Mishra (2019) and Mohan et al., (2019) investigated self-sustaining algal biorefinery design models with a closed-loop approach regarding the byproduct utilization in the system [11,12]. In particular, Mitra and Mishra (2019) discussed the current state of the art and potential advancements of a zero-waste biorefinery from *Arthrospira* spp. through the valorization of multiple products, such as biofertilizers, jet fuels, nutraceuticals, and c-phycocyanin, while Mohan et al., (2019) looked into the co-production of monomeric sugars, bioalcohols, and biohydrogen [11,12]. De Bhowmick et al., (2019) proposed biofuel and biochar co-production to minimize and possibly achieve net zero waste discharge [13]. Hemalatha et al., (2019) studied the potential of a microalgae biorefinery with a cascading resource recovery design through the integration of dairy wastewater treatment processes [14]. Wu and Chang (2019) evaluated an integrated microalgal biorefinery from a process systems engineering standpoint using life cycle assessment and techno-economic assessment methodologies to appraise the biorefinery's environmental and economic benefits [15]. However, the previously mentioned studies simply review the zero-waste concept applied to an algal biorefinery without mathematically supported decision making presented. The inherent complexity of designing biorefineries with several significantly interdependent processes requires appropriate systematic management tools, such as optimization modeling, to ensure that the potential benefits of closed-loop biorefineries are achieved, such as reduced resource consumption and waste or pollution generation, while minimizing any unintended negative consequences [16,17]. Looking specifically into optimization models on algal biorefineries, Garcia Prieto et al., (2017) developed a mixed integer nonlinear programming model for the design of an integrated algal biorefinery aiming to maximize its net present value [18]. However, the study only focused on a single objective involving economic impact, which indicates that their solution may not be environmentally sustainable. This has been addressed through a superstructure optimization model proposed by Gong and You (2014) covering algae cultivation, harvesting, drying, and lipid extraction to minimize costs and greenhouse gas emissions, achieving zero emissions throughout the process through reutilization [19]. The same reutilization of all wastes and products may be achieved with proper design. A multi-objective target-oriented robust optimization model was developed by Sy et al., (2018) for an integrated algal biorefinery polygeneration system focusing on profit maximization and environmental footprint minimization, which was later extended by Culaba et al., (2019) into a multi-period model to capture fluctuations in demand through planning periods and allow for material storage to buffer disparities between available supply and spikes in demand [16,17]. However, these studies did not take into account the specific inputs and outputs of each process in the integrated algal biorefinery by treating the algal biorefinery as a black box process unit. Each process within an algal biorefinery entails several potentially complicated and conflicting decisions that should also be taken into account. To address these, Ching et al., (2021) make use of artificial intelligence-based methodologies to model and possibly optimize the vacuum drying process of *Chlorococcum infusionum* for algal biofuel production [20]. Focusing instead on the cultivation and harvesting processes, San Juan et al., (2020) proposed a scheduling and planning optimization algorithm that maximizes profit and minimizes environmental impact through decisions such as species selection and cultivation and harvesting technology selection and scheduling [21]. Nonetheless, these processes within an algal biorefinery cannot only be modeled as stand-alone systems, under the assumption that no interaction exists between them. Accounting for interactions between these processes and other process systems that can operate symbiotically with algal biorefineries may be helpful in improving economic and environmental performances. A superstructure optimization model was formulated by Galanopoulos et al., (2019) integrating an algal biorefinery with a straw wheat biorefinery to minimize a single objective (i.e., biofuel production costs) [22]. Caligan et al., (2020) modeled the integration of a wastewater treatment plant and an algal biorefinery connected through the potential of cultivating algae on wastewater [23]. Extending this, San Juan et al., (2020) proposed a multi-objective optimization model to design an integrated system consisting of a wastewater treatment park, an algal biorefinery, and a sludge-based bioenergy conversion system [24]. Čuček et al., (2014) formulated a mixed integer linear programming model for the synthesis of a bioenergy supply network utilizing a combination of first-, second-, and third-generation biofuels (e.g., bioethanol, biohydrogen, and biodiesel) to maximize economic performance [25]. However, it is important to note that these systems do not feature a self-sustaining algal biorefinery because of their dependence on other supplementary systems. Integrating these facilities may not necessarily be practical when the facilities have already been established as stand-alone systems geographically far away from each other, as installing connections between them may be costly, inefficient, or impossible.

To be able to accurately calculate the environmental impact generated by a certain product, the life cycle assessment (LCA) methodology is used. According to the ISO 14040 standard, a full product life cycle is measured starting from the extraction of raw materials until the product end-of life. The LCA methodology has been applied to existing studies relating to algal biorefineries. Chowdhury et al., (2018) made use of the LCA methodology to simulate the effect of residence time on the production of algal bioenergy from dairy manure [26]. The LCA model developed was able to predict that with diluted waste and shorter residence time, energy requirement and greenhouse gas (GHG) emissions for the bioenergy production can be reduced. Moreover, Barlow et al., (2016) used the LCA methodology along with techno-economic assessment (TEA) to identify the sustainability of incorporating hydrothermal liquefaction and wastewater treatment into the algal biofuel production system [27]. It was determined that incorporating wastewater treatment into the system was able to reduce the environmental impact of the biorefinery. However, the LCA methodology simply provides an evaluation for a pre-determined system and cannot alone be used in system design.

The life cycle optimization (LCO) methodology was created to be able to integrate the advantages of the LCA methodology into an optimization model for application in system design. With the use of TEA and LCA methodologies, Wu et al., (2018) were able to develop an optimization model to obtain the optimal combination of cultivation and pretreatment process chains for an algal biorefinery [28]. The optimization model aimed to minimize environmental impact and maximize revenue. While having resource recirculation in the form of heat and CO_2 recovery, the study did not account for waste recovery and reuse for wastewater and biomass residue, which are possible sources of revenue and can lead to worsened environmental impact in the long run.

The LCA methodology is incorporated into this optimization model through the environmental optimization objective. In the previously mentioned study by Wu et al., (2018), the impact assessment method used was life cycle GHG emissions [28]. Bussa et al., (2018) stated that the ReCiPe impact assessment method is most recommended for microalgal biorefinery systems as it covers numerous environmental factors, not just concerning energy and greenhouse gas emissions [29]. Therefore, it was decided that the ReCiPe impact assessment method would be used for the life cycle optimization model.

Therefore, there is a need to develop a mathematical optimization model on an integrated microalgal biorefinery that optimizes profit and environmental impact, integrates the life cycle assessment methodology to account for the environmental impacts associated with a microalgal biofuel process flow, and incorporates resource recirculation among materials recirculated within the biorefinery centered on a closed-loop production system.

2. System Definition

The algal biorefinery featured in the study is divided into two main sections. The process units included in the first section are microalgae cultivation, harvest and dewatering, and lipid extraction, which are the upstream processes [30]. In this study, different process unit alternatives are selected for the upstream processes, and a comparison of each is presented in Table 1.

Table 1. Comparison of the different process unit alternatives.

Process	Alternative	Advantages	Disadvantages	Ref
Cultivation	Open pond	Low installation and operating costs	Varying culture conditions	[31]
	Photobioreactor	High control over culture parameters	High capital and operating costs	
Harvesting	Flocculation	Over 90% recovery; possibly low cost	Chemical contamination; longer settle time	[32]
	Filtration	70–90% recovery	High capital and operating costs	
	Centrifugation	Over 90% recovery; can utilize most algae species	Energy-intensive	
Extraction	Microwave	Around 90–95% yield with great quality	High operating cost; energy-intensive	[33]
	Solvent	Low-cost solvents	Large amount of solvent needed	

The second section includes the downstream processes of the biorefinery, the conversion of algal biomass into its intended end-products such as biodiesel, glycerol, biochar, and fertilizer. The main output of the oil extraction process is algal lipids turned into biodiesel and glycerol through transesterification [34]. Aside from that, waste is generated from the lipid extraction process in the form of solid and liquid algal biomass residues. These residues are converted into bioproducts such as biochar and fertilizer through pyrolysis and anaerobic digestion, respectively [16]. With the methane generated from the anaerobic digestion process, a link to a combined heat and power plant is established for conversion to power and heat with the aim of recirculation back to the biorefinery. The biorefinery process flow is presented in Figure 1. Aside from the main processes involving microalgal biofuel production, recovery process units are also incorporated into the system. These are added to incorporate resource recirculation into the biorefinery through the zero-waste concept. Process units such as microalgae cultivation, harvesting, and lipid extraction each have recovery processing alternatives that are to be decided by the optimization model. Moreover, model decisions are also made regarding the usage of resource recovery process units.

For the optimization model, the following cost components will be considered namely: investment costs, operating costs, material purchase costs, utility costs, and inventory costs. Investment costs refer to the initial capital expenses incurred to build the algal biorefinery process units expressed on a cost per process unit basis. Operating costs include labor, overhead, and material costs associated with each process unit expressed as a cost per time period. Material purchase costs are set for each material input that is used up in the production system, expressed as a cost per kg unit. Given that the optimization model considers multiple time periods, inventory costs are included for each material expressed as a periodic cost per kg material. Since all process units involved in the microalgal biorefinery are all assumed to be in a single facility, transportation costs are not considered in the optimization model. These cost components are deducted from the revenue streams which would be derived from the sale of products. Demand and selling price parameters are determined for the final end-products of the biorefinery and presented in Table A1, while cost parameters are presented in Tables A2 and A3 of the Appendix A.

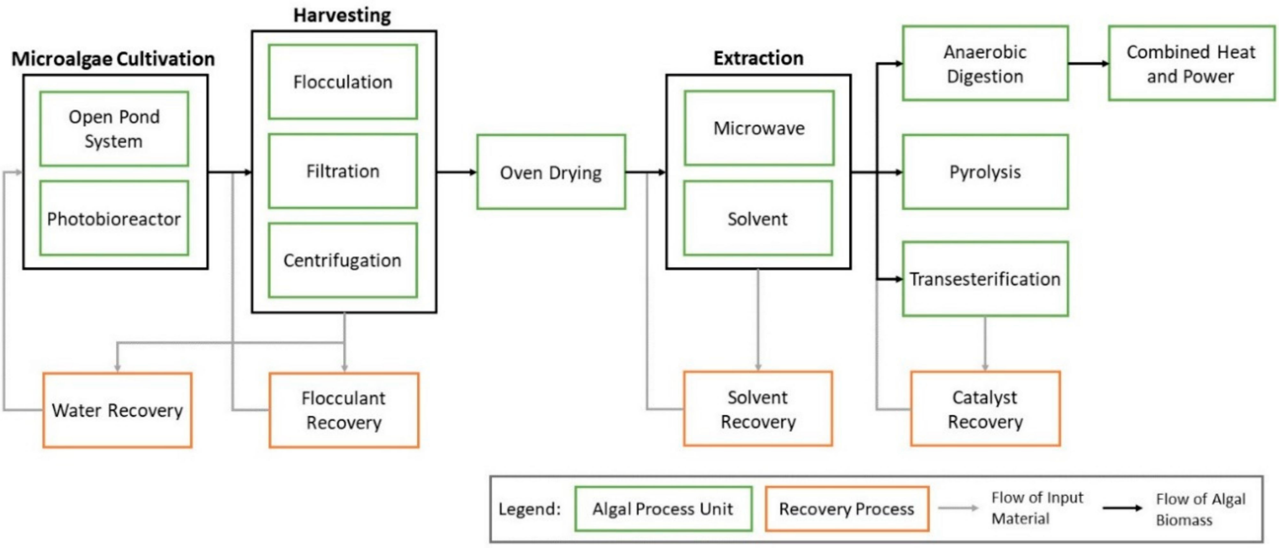

Figure 1. Algal biorefinery process flow.

The material inputs that are handled in resource recovery process units include water, solvent, flocculant, and catalyst. The optimization model involves multiple time periods to be able to incorporate the cyclability of resource recirculation. Furthermore, capital and operating costs are properly accounted for in the algal biorefinery with the consideration of multiple periods. For this study, a base period of 10 years will be used.

3. Life Cycle Assessment

For the environmental objective of the model, measures for environmental impact were obtained with the life cycle assessment (LCA) methodology. The goal of the study was to evaluate the total environmental impacts of each process path in the algal biorefinery. The system boundary of the study is presented in Figure 1. The study looked into each biorefinery product from its raw material extraction until its usage and end-of-life disposal scenarios. For LCA normalization, the functional unit to be utilized in the model was 1 kg biodiesel produced in the biorefinery. Various research articles such as those written by Gnansounou and Raman (2017), Dasan et al., (2019), Biller et al., (2013), Sy et al., (2018), Garcia Prieto et al., (2017), and Wu et al., (2018) were used as the basis for the material inputs and outputs as well as the energy consumption of each process unit [16,18,28,35–37]. After assessing the life cycle inventory, the researchers determined the overall impact of the system using the SimaPro software. For the impact assessment portion of the study, the ReCiPe 2016 Endpoint model was used in the simulation to be able to yield a single score impact value for each configuration in the microalgal production system. The environmental impact values generated from the LCA methodology were used as inputs for the objective function of the model to represent the environmental impact of each process path. Once a single score impact was determined for each production process configuration in the algal biorefinery, the one with the lowest single score was considered as the most sustainable configuration. However, this does not automatically mean that a certain configuration is optimal since a balance must be met between the economic and environmental objectives.

Data for the life cycle inventory for the different process paths are presented in Tables A4 and A5 of the Appendix A. Each process path was evaluated with a single score that represents its overall environmental impact. Impact categories were subject to normalization and weighting factors (see Table A6 of Appendix A) based on the ReCiPe 2016 method, aggregated to obtain the single score environmental impact. Looking firstly into upstream processes only, namely cultivation, harvesting, and oven drying, the resulting environmental impacts are presented in Figure 2. It is evident that the path with the greatest impact includes the photobioreactor cultivation and centrifugation for harvesting. The greatest contributor to this impact is the land use category due to the use of compost for cultivation and the larger input requirement for centrifugation. Moreover, it is seen that the upstream process with the highest contribution to environmental impact is centrifugation, attributable to its large biomass requirement for biodiesel production. On the other hand, the configuration with the least environmental impact is open pond cultivation paired with flocculation.

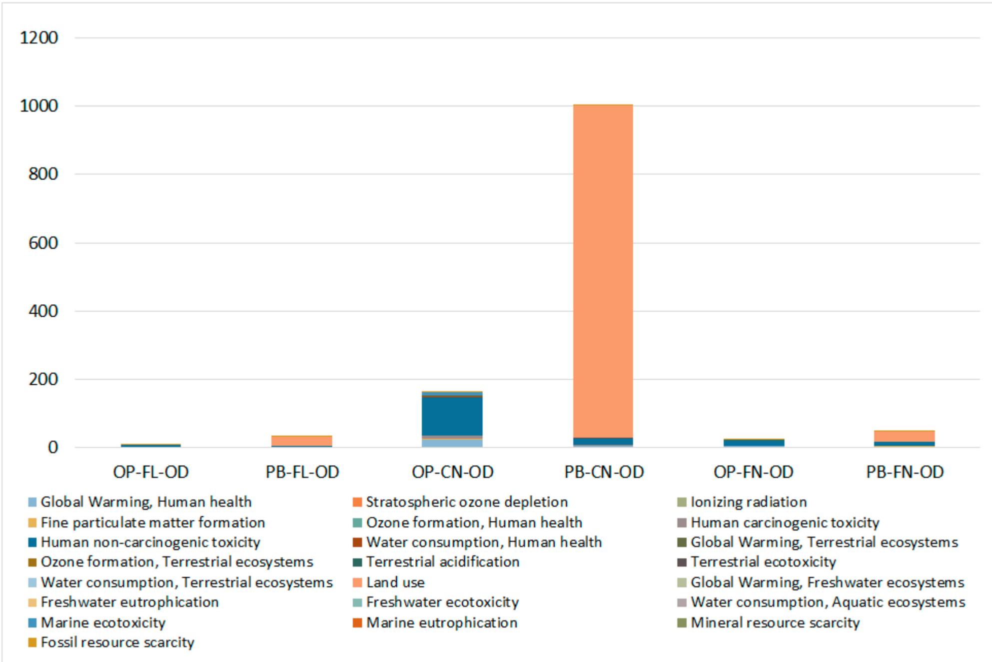

Figure 2. Life cycle environmental impacts of each upstream process path for 1 kg biodiesel (OP—open pond; PB—photobioreactor; FL—flocculation; CN—centrifugation; FN—filtration; OD—oven drying).

Consequently, the environmental impacts of the downstream process paths are displayed in Figure 3. The path with microwave extraction is shown to have the biggest environmental impact since it is more energy-intensive. The categories with the most contributions to the environmental impact of both scenarios are human non-carcinogenic toxicity and human health global warming attributable to the large energy requirements of anaerobic digestion.

Finally, looking into all process paths, the impacts are all displayed in Figure 4. The breakdown of environmental impacts for each process configuration and impact category is also numerically presented in Table A7 of the Appendix A. The paths with the largest environmental impact are those involving photobioreactor cultivation and centrifugation, since it is more energy-intensive. Similar to the earlier result, land use is the greatest contributor to the environmental impact values because of the use of compost for the nutrients used to cultivate the algal biomass. Among all the process paths, the one with the least impact is open pond cultivation with flocculation harvesting and solvent extraction, which makes it the most likely process path for the algal biorefinery.

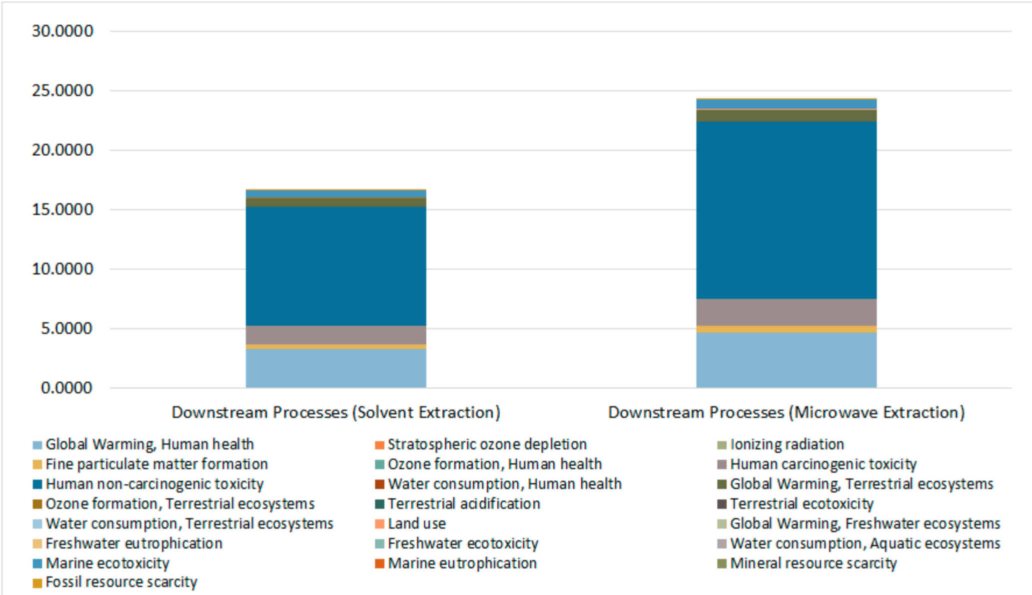

Figure 3. Life cycle environmental impacts of each downstream process path for 1 kg biodiesel.

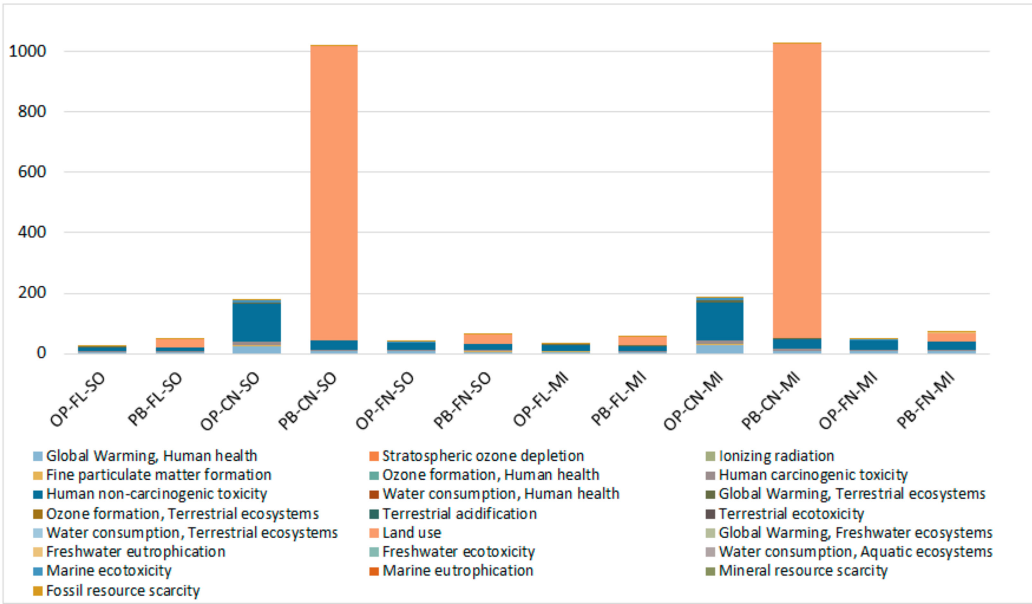

Figure 4. Life cycle environmental impacts of each process path for 1 kg biodiesel.

4. Model Formulation

A mixed integer linear programming (MILP) model was developed for the study with the objectives of optimizing the profit and environmental impacts while satisfying demand and capacity limitations. The indices, parameters, and variables are displayed in Tables A8–A10 of the Appendix A.

4.1. Model Assumptions

- All parameters considered in this model are deterministic and known with certainty.
- The outputs produced by the facility are transported to customers at the same time.
- Processing of algal biomass in all facilities is instantaneous.

4.2. Optimization Model

4.2.1. Objective Functions

The profit is calculated by working out the difference between the revenue generated from all products and the overall costs throughout the biorefinery, presented in Equation (1). Equation (2) defines the revenue for each period, which is computed by multiplying the selling price of each product by the total final outputs.

$$\text{Profit} = \sum\nolimits_t \text{Revenue}_t - \text{Total Cost} \tag{1}$$

$$\text{Revenue}_t = \sum\nolimits_p \sum\nolimits_t \text{SP}_{pt}\text{TO}_{pt} \tag{2}$$

The breakdown of the total costs is presented in Equation (3), which are investment costs, operating costs, material purchase costs, and inventory costs.

$$\text{Total Cost} = \text{Investment} + \sum\nolimits_t \text{Operating}_t + \sum\nolimits_t \text{Purchase}_t + \sum\nolimits_t \text{Inventory}_t \tag{3}$$

The total investment is the sum product of the fixed costs per process unit and the binary variable for selecting the alternative, presented in Equation (4). The operating costs for each period in the biorefinery are defined as the sum product of the operating costs per process and the corresponding product output, as shown in Equation (5).

$$\text{Investment} = \sum\nolimits_i \text{FC}_i\text{BC}_i + \sum\nolimits_j \text{FH}_j\text{BH}_j + \sum\nolimits_k \text{FE}_k\text{BE}_k + \sum\nolimits_r \text{FR}_r\text{BR}_r + \sum\nolimits_u \text{FP}_u\text{BP}_u \tag{4}$$

$$\begin{aligned}\text{Operating}_t = {} & \textstyle\sum_i \text{OC}_{it}\text{PC}_{it} + \sum_j \text{OH}_{jt}\text{PH}_{jt} + \sum_k \text{OE}_{kt}\text{PE}_{kt} + \sum_r \text{OR}_{rt}\text{PR}_{rt} \\ & + \textstyle\sum_u \text{OP}_{ut}\text{PP}_{ut}\end{aligned} \tag{5}$$

Equations (6) and (7) indicate the calculations for purchase and inventory costs, respectively. The material purchase costs are calculated by multiplying the purchase cost per input material with the total amount purchased each period. Meanwhile, the inventory costs are the unit storage costs for each input and output material and the total inventory level in each process unit.

$$\text{Purchase}_t = \sum\nolimits_m \text{MC}_{mt}\text{MQ}_{mt} \tag{6}$$

$$\text{Inventory}_t = \sum\nolimits_m \text{IC}_{mt}\text{EI}_{mt} \tag{7}$$

The environmental impact minimization objective is defined in Equation (8). It is the sum product of the environmental impact per output of each process unit and their corresponding total output.

$$\text{Impact} = \sum\nolimits_i \text{EC}_i\text{PC}_i + \sum\nolimits_j \text{EH}_j\text{PH}_j + \sum\nolimits_k \text{EE}_k\text{PE}_k + \sum\nolimits_r \text{ER}_r\text{PR}_r + \sum\nolimits_u \text{EP}_u\text{PP}_u \tag{8}$$

Since the model has dual objectives, there must be a balance between the economic and environmental objectives to generate the optimal solution. The objective function is defined as the maximization of the least desired value to balance the two objectives as seen in Equation (9) [38]. Equations (10) and (11) define the efficiencies for each objective, obtained by calculating the ratio of the attained improvement, which is the actual value subtracted from the worst possible one, and the potential improvement, which is the best possible value subtracted from the worst possible one. The best possible values for the two objectives are acquired through the optimization of each corresponding objective using a single objective linear programming model. The assumption is that the worst possible value for the environmental impact objective is its value when the profit objective is optimized, and vice versa.

$$\text{Max Z} = \min\left[\text{Eff}_{\text{Profit}}, \text{Eff}_{\text{Impact}}\right] \tag{9}$$

$$\text{Eff}_{\text{Profit}} = \frac{\text{Profit}_{\text{worst}} - \text{Profit}}{\text{Profit}_{\text{worst}} - \text{Profit}_{\text{best}}} \tag{10}$$

$$\text{Eff}_{\text{Impact}} = \frac{\text{Impact}_{\text{worst}} - \text{Impact}}{\text{Impact}_{\text{worst}} - \text{Impact}_{\text{best}}} \tag{11}$$

With the nonlinear nature of the objective function defined above, it is necessary to include linearizing constraints to the model to make sure that the optimization model generates the optimal solution. Equations (13) and (14) illustrate that the final value for efficiency is equal to the minimum of the efficiencies of the two objectives [38], while Equation (12) shows the final objective function.

$$\text{Max Z} = \text{Efficiency} \tag{12}$$

$$\text{Efficiency} \leq \text{EffProfit} \tag{13}$$

$$\text{Efficiency} \leq \text{EffImpact} \tag{14}$$

4.2.2. Constraints

The model constraints regarding the demand for the various products of the biorefinery are presented in Equation (15). The total amount of each product to be transported must be greater than or equal to the customer demand for each product, namely biodiesel, glycerol, biochar, and fertilizer.

$$\text{TO}_{\text{pt}} \geq \text{D}_{\text{pt}} \quad \forall \text{p} \quad \forall \text{t} \tag{15}$$

The capacity constraints define the production capability of each process as defined in Equations (16)–(20). The overall production output of each process is set to be less than or equal to the production capacity of that process unit multiplied by the binary variable assigned to each process.

$$\text{PC}_{\text{it}} \leq \text{BC}_{\text{i}} * \text{CC}_{\text{i}} \quad \forall \text{i} \quad \forall \text{t} \tag{16}$$

$$\text{PH}_{\text{jt}} \leq \text{BH}_{\text{j}} * \text{CH}_{\text{j}} \quad \forall \text{j} \quad \forall \text{t} \tag{17}$$

$$\text{PE}_{\text{kt}} \leq \text{BE}_{\text{k}} * \text{CE}_{\text{k}} \quad \forall \text{k} \quad \forall \text{t} \tag{18}$$

$$\text{PR}_{\text{rt}} \leq \text{BR}_{\text{r}} * \text{CR}_{\text{r}} \quad \forall \text{r} \quad \forall \text{t} \tag{19}$$

$$\text{PP}_{\text{ut}} \leq \text{BP}_{\text{u}} * \text{CP}_{\text{u}} \quad \forall \text{u} \quad \forall \text{t} \tag{20}$$

The product input-to-output conversion is defined in process constraints shown in Equations (21)–(26). For the conversion of product inputs to their corresponding outputs, the output of the previous process is set to be greater than or equal to the overall production output of the process multiplied by the conversion output yield.

$$\sum\nolimits_{\text{j}} \text{PH}_{\text{jt}}\text{YH}_{\text{j}} \leq \sum\nolimits_{\text{i}} \text{PC}_{\text{it}} \quad \forall \text{t} \tag{21}$$

$$\text{PP}_{\text{Dry,t}} * \text{YP}_{\text{Dry}} \leq \sum\nolimits_{\text{j}} \text{PH}_{\text{jt}} \quad \forall \text{t} \tag{22}$$

$$\sum\nolimits_{\text{k}} \text{PE}_{\text{kt}}\text{YE}_{\text{k}} \leq \text{PP}_{\text{Drying,t}} \quad \forall \text{t} \tag{23}$$

$$\text{PP}_{\text{Trans,t}} * \text{YP}_{\text{Trans}} \leq 0.6 * \sum\nolimits_{\text{k}} \text{PE}_{\text{kt}} \quad \forall \text{t} \tag{24}$$

$$\text{PP}_{\text{AD,t}} * \text{YP}_{\text{AD}} \leq 0.3 * \sum\nolimits_{\text{k}} \text{PE}_{\text{kt}} \quad \forall \text{t} \tag{25}$$

$$\text{PP}_{\text{Pyro,t}} * \text{YP}_{\text{Pyro}} \leq 0.1 * \sum\nolimits_{\text{k}} \text{PE}_{\text{kt}} \quad \forall \text{t} \tag{26}$$

$$\text{PP}_{\text{CHP,t}} * \text{YP}_{\text{CHP}} \leq 0.6 * \text{PP}_{\text{AD,t}} \quad \forall \text{t} \tag{27}$$

The equations regarding the relationships between the total final product outputs and the production outputs of the conversion processes are displayed in Equations (28)–(31).

The final product outputs are limited by the conversion efficiencies of their respective processes.

$$\mathrm{TO}_{\mathrm{Biodiesel},t} \leq 0.9 * \mathrm{PP}_{\mathrm{Trans},t} \quad \forall t \tag{28}$$

$$\mathrm{TO}_{\mathrm{Glycerol},t} \leq 0.1 * \mathrm{PP}_{\mathrm{Trans},t} \quad \forall t \tag{29}$$

$$\mathrm{TO}_{\mathrm{Biochar},t} \leq \mathrm{PP}_{\mathrm{Pyro},t} \quad \forall t \tag{30}$$

$$\mathrm{TO}_{\mathrm{Fertilizer},t} \leq 0.4 * \mathrm{PP}_{\mathrm{AD},t} \quad \forall t \tag{31}$$

As for the equations presenting how the production outputs of select processes branch out into inputs and outputs of corresponding next processes, they are displayed in Equations (32)–(34). Equation (32) details the flow of materials from the extraction processes into the anaerobic digestion, pyrolysis, and transesterification process units. Similarly, Equation (33) describes biodiesel and glycerol to be the product outputs of the transesterification process, while the outputs of the anaerobic digestion unit include the final product fertilizer and inputs into combined heat and power process unit.

$$\textstyle\sum_k \mathrm{PE}_{kt} \geq \mathrm{PP}_{\mathrm{Trans},t} * \mathrm{YP}_{\mathrm{Trans}} + \mathrm{PP}_{\mathrm{AD},t} * \mathrm{YP}_{\mathrm{AD}} + \mathrm{PP}_{\mathrm{Pyro},t} * \mathrm{YP}_{\mathrm{Pyro}} \quad \forall t \tag{32}$$

$$\mathrm{PP}_{\mathrm{Trans},t} \geq \mathrm{TO}_{\mathrm{Biodiesel},t} + \mathrm{TO}_{\mathrm{Glycerol},t} \quad \forall t \tag{33}$$

$$\mathrm{PP}_{\mathrm{AD},t} \geq \mathrm{TO}_{\mathrm{Fertilizer},t} + \mathrm{PP}_{\mathrm{CHP},t} * \mathrm{YP}_{\mathrm{CHP}} \quad \forall t \tag{34}$$

The relationship between the recovered material inputs in each facility and the respective material input usage in production for each facility is presented in Equations (35)–(38). Equations (35) and (36) model the recovery of water and flocculant from harvesting, respectively, while Equation (37) represents the recovery of solvent from the extraction process alternatives. The same is done for the recovery of catalyst from the transesterification process in Equation (38).

$$\textstyle\sum_j \mathrm{PH}_{jt}\mathrm{YH}_j \geq 0.9 * \mathrm{PR}_{\mathrm{Water},t} \quad \forall t \tag{35}$$

$$\textstyle\sum_j \mathrm{PH}_{jt}\mathrm{YH}_j \geq 0.05 * \mathrm{PR}_{\mathrm{Floc},t} \quad \forall t \tag{36}$$

$$\textstyle\sum_k \mathrm{PE}_{kt}\mathrm{YE}_k \geq 0.1 * \mathrm{PR}_{\mathrm{Solv},t} \quad \forall t \tag{37}$$

$$\mathrm{PP}_{\mathrm{Trans},t} * \mathrm{YP}_{\mathrm{Trans}} \geq 0.2 * \mathrm{PR}_{\mathrm{Cat},t} \quad \forall t \tag{38}$$

Equations (39)–(42) describe the flow of the material inventory in the system understudy. The beginning inventory is defined in Equation (39) as a function of material purchases and the ending inventory carried over from the previous period, while the ending inventory is expressed as a function of the beginning inventory and recovered material inputs in Equation (40). Equations (41) and (42) ensure that the amount of material purchased and kept inventory are limited by the available inventory and purchase capacities.

$$\mathrm{BI}_{mt} = \mathrm{MQ}_{mt} + \mathrm{EI}_{mt-1} \quad \forall t \tag{39}$$

$$\mathrm{EI}_{mt} = \mathrm{BI}_{mt} + \mathrm{PR}_{mt} \quad \forall t \tag{40}$$

$$\mathrm{EI}_{mt} \leq \mathrm{IK}_{mt} \quad \forall t \tag{41}$$

$$\mathrm{MQ}_{mt} \leq \mathrm{MK}_{mt} \quad \forall t \tag{42}$$

The available material inputs (i.e., water, flocculant, solvent, and catalyst) at the beginning of each period should be able to satisfy the requirements of their respective conversion processes (i.e., cultivation, harvesting, extraction, and transesterification). These constraints are modeled in Equations (43)–(46).

$$\mathrm{BI}_{\mathrm{Water},t} \geq 0.9 * \textstyle\sum_i \mathrm{PC}_{it}\mathrm{YC}_i \quad \forall t \tag{43}$$

$$BI_{Floc,t} \geq 0.05 * \sum_j PH_{jt} YH_j \quad \forall t \tag{44}$$

$$BI_{Solv,t} \geq 0.1 * \sum_k PE_{kt} YE_k \quad \forall t \tag{45}$$

$$BI_{Cat,t} \geq 0.2 * PP_{Trans,t} * YP_{Trans} \quad \forall t \tag{46}$$

Equations (47)–(49) require that the system activates one of the available alternatives in each of the cultivation, harvesting, and extraction processes, while Equation (50) ensures that other processes without alternative units must be installed through binary constraints.

$$\sum_i BC_i = 1 \tag{47}$$

$$\sum_j BH_j = 1 \tag{48}$$

$$\sum_k BE_k = 1 \tag{49}$$

$$BP_u = 1 \quad \forall u \tag{50}$$

5. Model Validation

The mathematical optimization model was validated with the use of MATLAB R2020a software along with the Cplex optimization solver. A base case is considered as an initial scenario to be used for comparison in the scenario analysis. In order to attain the best and worst possible values involving the two objectives which were used in calculating the efficiency, optimization with single objectives was executed.

5.1. Profit Maximization

With the objective of profit maximization, the algal biorefinery chose to operate at its maximum yielding annual biodiesel output of 49,473.14 kg. The optimal selection of process alternatives with only profit consideration for cultivation, harvesting, and extraction is shown in Figure 1. Based on the results, the process units chosen were those that require the least fixed cost among other alternatives, which were open pond cultivation, centrifugation harvesting, and solvent extraction. However, the maximized production of biodiesel results in a trade-off for the environmental impact objective since this process configuration is one of those with the biggest impact as calculated from the LCA methodology.

5.2. Impact Minimization

Consequently, looking into the environmental objective, biodiesel production was performed only to meet the minimum annual demand of 25,000 kg. A larger production amount would result in a higher impact given that the single score values are calculated based on a unit output for each process. Figure 1 presents the process path that yields the least environmental impact as calculated from the life cycle assessment. However, the resulting profit value with this process flow drastically changes, resulting in a net loss (see Table 2) given that the revenue generated is lower than the total production cost since less biofuel and other bioproducts are produced from the microalgal biorefinery.

Table 2. Summary of single objective optimization results.

	Maximized Profit	Minimized Impact
Overall Profit—10 Periods (USD)	5,923,239.93	−36,518.68
Annual Impact (kPt)	8,682.01	592.40
Annual Biodiesel Output (kg)	48,977.79 kg	25,000 kg

The results presented above validate the hypothesis that a balance must be established between the two objectives to obtain the optimal result. With that, the developed model with the efficiency objectives highlighted in the model formulation section were added onto the final model.

5.3. Multi-Objective Model

Using the obtained results from the single-objective execution of the optimization model, the best and worst values for the profit and environmental impact were retrieved. With that, the efficiency could be calculated for both objectives which was then maximized for the optimization model.

The resulting optimal efficiency value obtained from the model was 92.69%, as presented in Table 3, which means that the optimal multi-objective values are very close to their respective single objective values. Annual biodiesel production equates to 49,951.43 kg, which is higher than that of the first two single-objective runs while having a lower profit than the maximum profit single objective. This shows the significance of incorporating certain process paths in the system. Looking simply into the economic objective, a bigger profit is achieved with less output due to the use of low-cost processes. Figure 1 shows the optimal process path chosen for the biorefinery, which is identical to that of the minimum impact single objective. This shows the balance that was established between the two objectives to yield the optimal result.

Table 3. Summary of multi-objective optimal results.

	Optimal Value	Efficiency
Overall Profit—10 Periods (USD)	5,487,668.69	92.69%
Annual Impact (kPt)	1183.65	92.69%
Annual Biodiesel Output (kg)	49,951.43	-

Looking into the behavior of product purchasing given the incorporation of the recovery processes, purchase amounts for each product are presented in Figure 5.

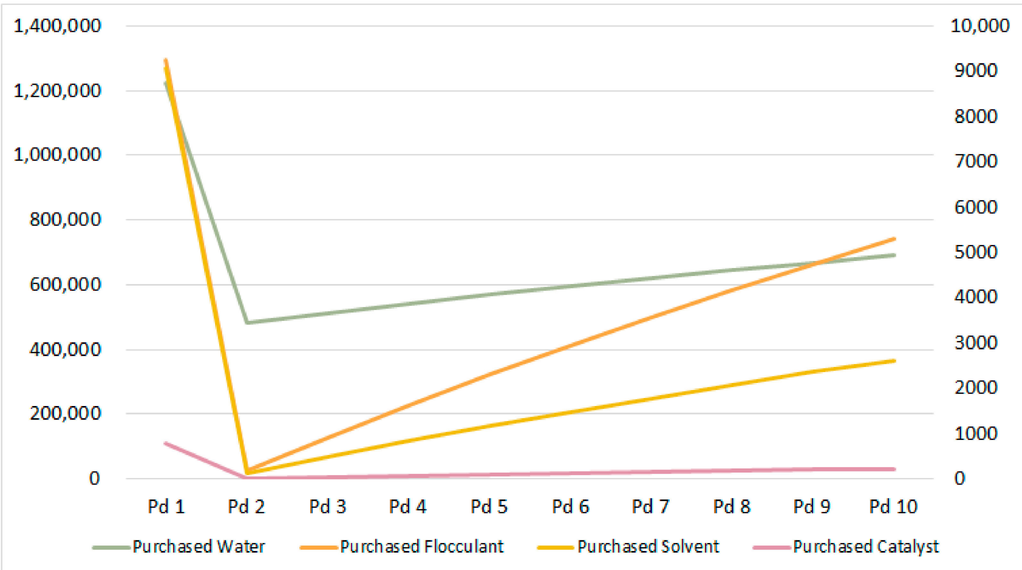

Figure 5. Behavior of purchase amounts for each input material over time.

For the first period, the maximum purchase amounts are seen since there is no initial inventory count and no material recovered yet. By the second year, due to the recovered materials from the previous period, a decrease in the purchase amount is observed. However, since the recovery efficiency decreases over time, purchase amounts start to increase after the second year. This behavior is beneficial to the algal biorefinery due to the purchase cost savings and an overall decrease in use of new materials. To discuss further, the inventory level of each material over time is assessed, as presented in Figure 6.

It can be observed that the behaviors of the purchase amounts and inventory levels of each material follow an inverse relationship. The inventory rose to maximum levels during the second period due to the newly recovered materials from the first period. Moreover, the inventory started to decrease, attributable to the decreasing efficiency level of the recovery processes. Eventually, the inventory of materials would reach a minimum, which would then indicate that a full purchase of new materials is needed.

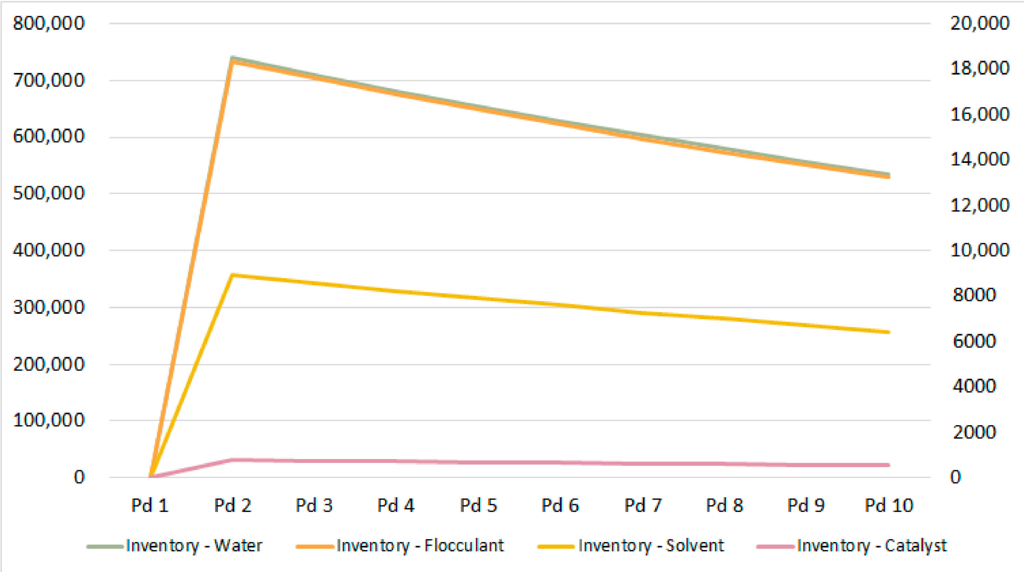

Figure 6. Behavior of inventory levels for each input material over time.

6. Scenario Analysis

To assess the capabilities of the optimization model further, a scenario analysis was conducted looking into the impacts of applying efficiencies to each process unit and fluctuations in demand for biodiesel.

6.1. Impact of Process Unit Efficiencies

For the base case, it was assumed that all process units are always 100% efficient. However, this is not true most of the time due to the occurrence of waste and differences in raw material input quality. To look into the effect of the application of efficiencies to each process unit, different efficiency levels were assigned to all process units to test the corresponding impact on the objective functions. An efficiency level lower than 100% indicates that a unit of input yields less output compared to its full capacity.

Decreasing the efficiency levels of each process unit yields less environmental impact and less profit for the algal biorefinery (see Figure 7a). Although the decrease in impact is favorable, the decrease in profit is not. This behavior occurs since less products are produced within the system, which yields less revenue and overall environmental impact. Aside from that, it is noted that the efficiency objective functions which are related to the worst and best values for each of the objectives have an inverse relationship with the process unit efficiencies, as seen in Figure 7b. This indicates that the resulting optimal values from the multi-objective model move nearer to the optimal results from the single-objective runs for each objective as efficiency decreases. However, this is not a favorable outcome if looking at the big picture since the profit has an opposite trend.

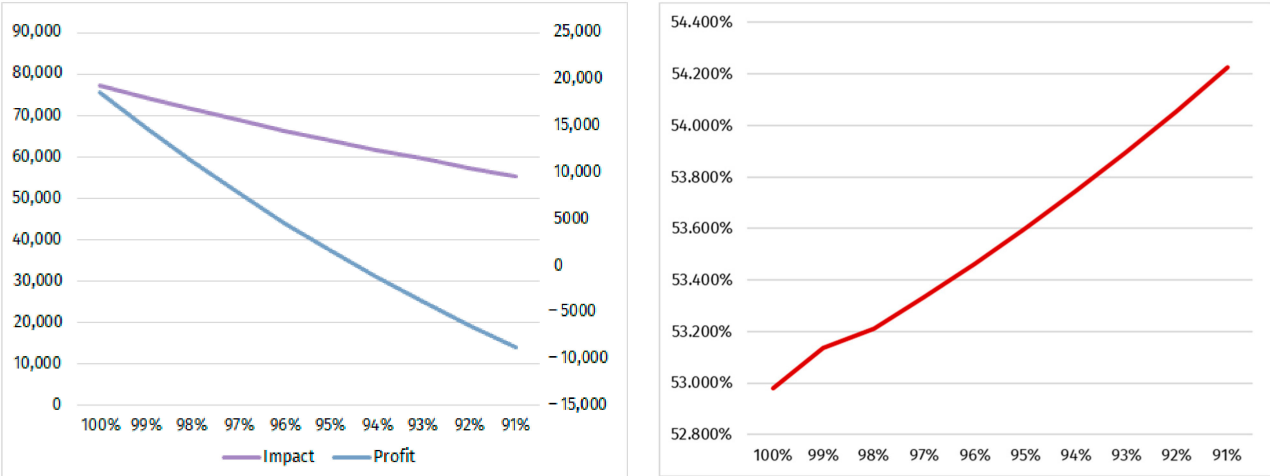

(**a**) (**b**)

Figure 7. Results under varying process unit efficiencies: (**a**) Profit and environmental impact optimal values under varying process efficiencies; (**b**) objective function efficiency values under varying process efficiencies.

6.2. Impact of Demand Fluctuations

Product demand does not always assume a deterministic value. Most of the time, fluctuations in demand are caused by various industry factors affecting the operations of the production line. To determine the impact when accounting for demand fluctuations, a demand index, taking values from 1.5 to 0.5 at an interval of 0.1, was incorporated to be multiplied to the current demand parameter to represent the changes in demand. The results of the optimization model with the adapted fluctuations in demand are presented in Figure 8a,b.

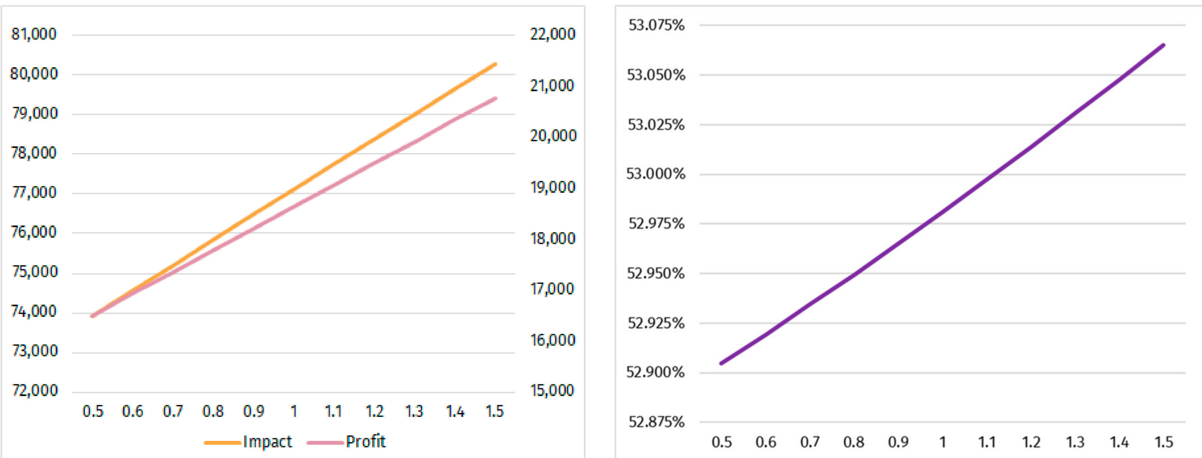

(**a**) (**b**)

Figure 8. Results under varying demand parameters: (**a**) Profit and environmental impact optimal values under varying demand; (**b**) objective function efficiency values under varying demand.

A higher demand, as represented by the demand indices ranging 1.5 to 1.1, indicates higher production of biodiesel, which leads to a higher profit and environmental impact (see Figure 8a). A similar trend is seen with regards to having a lower demand. This indicates that the objective values are highly sensitive to the demand parameters that are set in the model. The varying demand parameters come with changes in the efficiency objective values as seen in Figure 8b. A higher demand setting yields a higher efficiency value since the denominator for the profit efficiency, which is the potential improvement for profit, takes on a lower value. This is because the worst possible profit is increased due to taking on a bigger demand. With lower demand comes the lower worst possible profit value, which then results in a decrease in the efficiency objective value. This is an indicator that the demand estimate for the base case may have been too low for the system. This shows the importance of appropriate demand forecasting alongside a system that is able to overcome demand fluctuations.

7. Conclusions and Recommendations

This study introduced a multi-objective optimization model for an algal biorefinery incorporating a circular bioeconomy outlook with objectives of maximizing profit and minimizing environmental impact. To determine the single score impact assessment for the process units involved in the system boundary, a life cycle analysis (LCA) methodology was utilized, looking into the life cycle of the products from cultivation until usage and disposal. Incorporating this technique into the optimization model created a new approach in determining the environmental impact associated with each product to be applied in mathematical modeling. The model aimed to design a system for an algal biorefinery to determine which processes to take in to consideration.

By looking into the profit and environmental impact objectives separately through single-objective optimization, the conflict between the two was observed through their inverse relationship. When profit maximization is prioritized, the resulting environmental impact increases, which is unfavorable due to the harm it will cause for the environment. On the other hand, when environmental impact is minimized, the algal biorefinery obtains a net loss since the generated revenue is not enough to cover the overall production expenses. Considering both objectives simultaneously through the optimization model would strike a balance between profit and environmental impact for the algal biorefinery.

Consideration of process unit efficiencies as well as demand fluctuations causes significant changes in the objective function values. A lower process unit efficiency results in a decrease in profit and impact due to less product outputs. Similarly, having a lower demand parameter yields less profit and environmental impact since biodiesel production is decreased. This shows the impact of the changes in demand and process unit efficiencies that are usually caused by numerous other factors outside the system.

A possible extension of this research may be through the incorporation of uncertain parameters into the optimization model such as demand, microalgae nutrient content, and process unit product yield. The LCA section of the study currently lacks further investigation on the breakdown of environmental impacts in each process. A more in-depth analysis on the results of the LCA methodology can also be added to the research, expounding on the impacts of specific material inputs in the algal biorefinery. Moreover, using real-life data for the estimating system parameters would lead to more accurate findings for applied industry projects.

Author Contributions: Conceptualization, C.M.A.S., J.L.G.S.J., and A.P.M.; model formulation, verification, and validation, C.M.A.S.; writing—original draft preparation, C.M.A.S.; writing—review and editing, J.L.G.S.J., A.P.M., C.L.S., A.T.U., and A.B.C. All authors have read and agreed to the published version of the manuscript.

Funding: This research received no external funding.

Conflicts of Interest: The authors declare no conflict of interest.

Appendix A

Table A1. Demand and selling price for each product [16].

	Demand (kg)	Selling Price (USD/kg)
Biodiesel	25,000	12.50
Glycerol	2500	0.78
Biochar	1000	0.50
Fertilizer	200	0.25

Table A2. Purchase and inventory costs for each recoverable material [18].

	Purchase Cost (USD/kg)	Inventory Cost (USD/kg/pd)
Water	0.367	0.15
Potassium sulfate	0.12	0.15
Hexane	0.41	0.15
Sulfuric acid	0.74	0.15

Table A3. Fixed and operating costs for each process unit [16,18,36].

	Fixed Cost (USD)	Operating Cost (USD)
Open Pond	734,713.76	0.50
Photobioreactor	1,192,058.79	0.50
Flocculation	923,823.86	0.50
Centrifugation	285,617.51	0.50
Filtration	807,400.00	0.50
Oven Drying	632,120.00	0.50
Solvent Extraction	720,000.00	0.50
Microwave Extraction	936,000.00	0.50
Transesterification	1,050,441.71	0.50
Pyrolysis	357,760	0.50
Anaerobic Digestion	693,600	0.50
Combined Heat and Power	459,000	0.25

Table A4. Life cycle inventory for 1 kg of biodiesel (open pond systems) [15,16,18,35–37].

Stages	Material	OP-FL-SO	OP-CN-SO	OP-FN-SO	OP-FL-MI	OP-CN-MI	OP-FN-MI
Cultivation—Open Pond	Water (kg)	6.4852	221.7602	6.3385	1.7546	59.9993	1.7150
	Urea (g)	2.5779	88.1497	2.5196	0.6975	23.8497	0.6817
	Diammonium phosphate (g)	2.3185	79.2793	2.2660	0.6273	21.4498	0.6131
	Electricity (MJ)	0.3599	12.3077	0.3518	0.0974	3.3300	0.0952
	* Algal broth (kg)	6.6203	226.3802	6.4706	1.7912	61.2493	1.7507
Harvesting—Flocculation	Potassium sulfate (kg)	0.0794			0.0215		
	Electricity (MJ)	7.7385			2.0937		
	Algal broth (kg)	6.6203			1.7912		
	* Wet biomass (kg)	5.4353			1.4706		
Harvesting—Centrifugation	Chitosan (g)		45.9690			12.4374	
	Electricity (MJ)		12.4740			3.3750	
	Algal broth (kg)		226.3802			61.2493	
	* Wet biomass (kg)		5.4353			1.4706	
Harvesting—Filtration	Electricity (MJ)			190.2355			51.4700
	Algal broth (kg)			6.4706			1.7507
	* Wet biomass (kg)			5.4353			1.4706

Table A4. *Cont.*

Stages	Material	OP-FL-SO	OP-CN-SO	OP-FN-SO	OP-FL-MI	OP-CN-MI	OP-FN-MI
Oven Drying	Wet biomass (kg)	5.4353	5.4353	5.4353	1.4706	1.4706	1.4706
	Heat (MJ)	62.4516	62.4516	62.4516	16.8969	16.8969	16.8969
	* Dry biomass (kg)	4.6200	4.6200	4.6200	1.2500	1.2500	1.2500
Extraction—Solvent	Hexane (g)	2.9568	2.9568	2.9568			
	Electricity (MJ)	0.3326	0.3326	0.3326			
	Heat (MJ)	2.3100	2.3100	2.3100			
	Dry biomass (kg)	4.6200	4.6200	4.6200			
	* Algal oil (g)	1049.9884	1049.9884	1049.9884			
	* Liquid residue (g)	170.0000	170.0000	170.0000			
	* Solid residue (g)	40.0000	40.0000	40.0000			
Extraction—Microwave	Electricity (MJ)				36.7496	36.7496	36.7496
	Dry biomass (kg)				1.2500	1.2500	1.2500
	* Algal oil (kg)				1.0500	1.0500	1.0500
	* Liquid residue (g)				45.9951	45.9951	45.9951
	* Solid residue (g)				10.8224	10.8224	10.8224
Transesterification	Algal oil (g)	1049.9884	1049.9884	1049.9884	1049.9884	1049.9884	1049.9884
	Methanol (g)	124.8787	124.8787	124.8787	124.8787	124.8787	124.8787
	Sodium hydroxide (g)	10.4874	10.4874	10.4874	10.4874	10.4874	10.4874
	Sulfuric acid (g)	15.8004	15.8004	15.8004	15.8004	15.8004	15.8004
	Electricity (MJ)	0.1663	0.1663	0.1663	0.1663	0.1663	0.1663
	Heat (MJ)	5.5902	5.5902	5.5902	5.5902	5.5902	5.5902
	Water (kg)	0.1386	0.1386	0.1386	0.1386	0.1386	0.1386
	* Biodiesel (g)	1000.0000	1000.0000	1000.0000	1000.0000	1000.0000	1000.0000
	* Glycerol (g)	113.2825	113.2825	113.2825	113.2825	113.2825	113.2825
Pyrolysis	Solid residue (g)	40.0000	40.0000	40.0000	10.8224	10.8224	10.8224
	Heat (MJ)	6.4168	6.4168	6.4168	1.7361	1.7361	1.7361
	* Biochar (g)	5.9970	5.9970	5.9970	1.6225	1.6225	1.6225
Anaerobic Digestion	Liquid residue (g)	170.0000	170.0000	170.0000	45.9951	45.9951	45.9951
	Electricity (MJ)	54.7260	54.7260	54.7260	14.8066	14.8066	14.8066
	Heat (MJ)	416.2671	416.2671	416.2671	112.6250	112.6250	112.6250
	* Methane (g)	19.4064	19.4064	19.4064	5.2506	5.2506	5.2506
	* Fertilizer (g)	69.8428	69.8428	69.8428	18.8966	18.8966	18.8966
Combined Heat and Power	Methane (g)	19.4064	19.4064	19.4064	5.2506	5.2506	5.2506
	* Electricity (MJ)	0.2156	0.2156	0.2156	0.0583	0.0583	0.0583
	* Heat (MJ)	0.4097	0.4097	0.4097	0.1108	0.1108	0.1108

* Output Material; OP—Open Pond; FL—Flocculation; CN—Centrifugation; FN—Filtration; SO—Solvent; MI—Microwave.

Table A5. Life cycle inventory for 1 kg of biodiesel (photobioreactor) [15,16,18,35–37].

Stages	Input	PB-FL-SO	PB-CN-SO	PB-FN-SO	PB-FL-MI	PB-CN-MI	PB-FN-MI
Cultivation—Open Pond	Water (kg)	5.6105	191.8476	5.4836	1.5180	51.9062	1.4836
	Chicken compost (kg)	0.2244	7.6739	0.2193	0.0607	2.0762	0.0593
	Atmospheric air (kg)	0.2244	7.6739	0.2193	0.0607	2.0762	0.0593
	Inoculum (kg)	0.5610	19.1848	0.5484	0.1518	5.1906	0.1484
	Electricity (MJ)	5.5890	191.1152	5.4626	1.5122	51.7080	1.4780
	* Algal broth (kg)	6.6203	226.3802	6.4706	1.7912	61.2493	1.7507
Harvesting—Flocculation	Potassium sulfate (kg)	0.0794			0.0215		
	Electricity (MJ)	7.7385			2.0937		
	Algal broth (kg)	6.6203			1.7912		
	* Wet biomass (kg)	5.4353			1.4706		
Harvesting—Centrifugation	Chitosan (g)		45.9690			12.4374	
	Electricity (MJ)		12.4740			3.3750	
	Algal broth (kg)		226.3802			61.2493	
	* Wet biomass (kg)		5.4353			1.4706	

Table A5. *Cont.*

Stages	Input	PB-FL-SO	PB-CN-SO	PB-FN-SO	PB-FL-MI	PB-CN-MI	PB-FN-MI
Harvesting—Filtration	Electricity (MJ)			190.2355			51.4700
	Algal broth (kg)			6.4706			1.7507
	* Wet biomass (kg)			5.4353			1.4706
Oven Drying	Wet biomass (kg)	5.4353	5.4353	5.4353	1.4706	1.4706	1.4706
	Heat (MJ)	62.4516	62.4516	62.4516	16.8969	16.8969	16.8969
	* Dry biomass (kg)	4.6200	4.6200	4.6200	1.2500	1.2500	1.2500
Extraction—Solvent	Hexane (g)	2.9568	2.9568	2.9568			
	Electricity (MJ)	0.3326	0.3326	0.3326			
	Heat (MJ)	2.3100	2.3100	2.3100			
	Dry biomass (kg)	4.6200	4.6200	4.6200			
	* Algal oil (g)	1049.9884	1049.9884	1049.9884			
	* Liquid residue (g)	170.0000	170.0000	170.0000			
	* Solid residue (g)	40.0000	40.0000	40.0000			
Extraction—Microwave	Electricity (MJ)				36.7496	36.7496	36.7496
	Dry biomass (kg)				1.2500	1.2500	1.2500
	* Algal oil (kg)				1.0500	1.0500	1.0500
	* Liquid residue (g)				45.9951	45.9951	45.9951
	* Solid residue (g)				10.8224	10.8224	10.8224
Transesterification	Algal oil (g)	1049.9884	1049.9884	1049.9884	1049.9884	1049.9884	1049.9884
	Methanol (g)	124.8787	124.8787	124.8787	124.8787	124.8787	124.8787
	Sodium hydroxide (g)	10.4874	10.4874	10.4874	10.4874	10.4874	10.4874
	Sulfuric acid (g)	15.8004	15.8004	15.8004	15.8004	15.8004	15.8004
	Electricity (MJ)	0.1663	0.1663	0.1663	0.1663	0.1663	0.1663
	Heat (MJ)	5.5902	5.5902	5.5902	5.5902	5.5902	5.5902
	Water (kg)	0.1386	0.1386	0.1386	0.1386	0.1386	0.1386
	* Biodiesel (g)	1000.0000	1000.0000	1000.0000	1000.0000	1000.0000	1000.0000
	* Glycerol (g)	113.2825	113.2825	113.2825	113.2825	113.2825	113.2825
Pyrolysis	Solid residue (g)	40.0000	40.0000	40.0000	10.8224	10.8224	10.8224
	Heat (MJ)	6.4168	6.4168	6.4168	1.7361	1.7361	1.7361
	* Biochar (g)	5.9970	5.9970	5.9970	1.6225	1.6225	1.6225
Anaerobic Digestion	Liquid residue (g)	170.0000	170.0000	170.0000	45.9951	45.9951	45.9951
	Electricity (MJ)	54.7260	54.7260	54.7260	14.8066	14.8066	14.8066
	Heat (MJ)	416.2671	416.2671	416.2671	112.6250	112.6250	112.6250
	* Methane (g)	19.4064	19.4064	19.4064	5.2506	5.2506	5.2506
	* Fertilizer (g)	69.8428	69.8428	69.8428	18.8966	18.8966	18.8966
Combined Heat and Power	Methane (g)	19.4064	19.4064	19.4064	5.2506	5.2506	5.2506
	* Electricity (MJ)	0.2156	0.2156	0.2156	0.0583	0.0583	0.0583
	* Heat (MJ)	0.4097	0.4097	0.4097	0.1108	0.1108	0.1108

* Output Material; PB—Photobioreactor; FL—Flocculation; CN—Centrifugation; FN—Filtration; SO—Solvent; MI—Microwave.

Table A6. Normalization and weighting factors for ReCiPe 2016 impact categories.

Category	Normalization Factor	Weighting Factor
Damage to human health	11.2	400
Damage to ecosystems	1186	400
Damage to resource availability	0.000357	200

Retrieved from SimaPro ReCiPe 2016 Egalitarian impact assessment method.

Table A7. Life cycle assessment results for 1 kg of biodiesel.

Impact Category	**OP-FL-SO**	**OP-CN-SO**	**OP-FN-SO**	**OP-FL-MI**	**OP-CN-MI**	**OP-FN-MI**	**PB-FL-SO**	**PB-CN-SO**	**PB-FN-SO**	**PB-FL-MI**	**PB-CN-MI**	**PB-FN-MI**
Global Warming, Human health	4.4227	3.9009	24.8744	7.0341	6.3919	5.8820	5.7478	5.2261	26.1995	8.3593	7.7171	7.2071
Stratospheric ozone depletion	1.79×10^{-4}	5.37×10^{-3}	1.42×10^{-3}	1.79×10^{-1}	2.83×10^{-4}	5.36×10^{-3}	2.35×10^{-4}	5.43×10^{-3}	1.48×10^{-3}	1.79×10^{-1}	3.39×10^{-4}	5.42×10^{-3}
Ionizing radiation	1.14×10^{-4}	7.14×10^{-5}	2.01×10^{-3}	5.75×10^{-4}	1.39×10^{-4}	9.79×10^{-5}	1.33×10^{-4}	9.05×10^{-5}	2.03×10^{-3}	5.94×10^{-4}	1.58×10^{-4}	1.17×10^{-4}
Fine particulate matter formation	0.5600	0.4905	3.3394	0.9656	0.8982	0.8303	0.7441	0.6747	3.5236	1.1497	1.0824	1.0145
Ozone formation, Human health	7.96×10^{-4}	7.66×10^{-4}	3.85×10^{-3}	2.81×10^{-3}	1.18×10^{-3}	1.15×10^{-3}	1.05×10^{-3}	1.02×10^{-3}	4.10×10^{-3}	3.06×10^{-3}	1.43×10^{-3}	1.40×10^{-3}
Human carcinogenic toxicity	2.1092	1.8749	12.1635	4.1494	3.6177	3.3886	2.8535	2.6191	12.9078	4.8936	4.3619	4.1329
Human non-carcinogenic toxicity	14.7170	11.9791	122.8033	29.1829	24.7466	22.0706	19.5436	16.8058	127.6299	34.0095	29.5732	26.8973
Water consumption, Human health	7.01×10^{-3}	5.32×10^{-4}	2.28×10^{-1}	6.33×10^{-3}	6.93×10^{-3}	5.98×10^{-4}	7.12×10^{-3}	6.44×10^{-4}	2.28×10^{-1}	6.44×10^{-3}	7.04×10^{-3}	7.10×10^{-4}
Global Warming, Terrestrial ecosystems	0.9381	0.8274	5.2763	1.4894	1.3536	1.2454	1.2188	1.1080	5.5569	1.7700	1.6343	1.5260
Ozone formation, Terrestrial ecosystems	1.21×10^{-2}	1.20×10^{-2}	5.90×10^{-2}	5.58×10^{-2}	1.79×10^{-2}	1.78×10^{-2}	1.58×10^{-2}	1.57×10^{-2}	6.28×10^{-2}	5.95×10^{-2}	2.17×10^{-2}	2.16×10^{-2}
Terrestrial acidification	5.06×10^{-2}	4.34×10^{-2}	3.28×10^{-1}	8.29×10^{-2}	7.14×10^{-2}	6.44×10^{-2}	6.51×10^{-2}	5.79×10^{-2}	3.43×10^{-1}	9.74×10^{-2}	8.60×10^{-2}	7.89×10^{-2}
Terrestrial ecotoxicity	8.60×10^{-4}	3.99×10^{-4}	1.71×10^{-2}	1.33×10^{-3}	1.02×10^{-3}	5.69×10^{-4}	9.86×10^{-4}	5.24×10^{-4}	1.72×10^{-2}	1.45×10^{-3}	1.14×10^{-3}	6.94×10^{-4}
Water consumption, Terrestrial ecosystems	4.70×10^{-3}	7.04×10^{-4}	1.47×10^{-1}	1.08×10^{-2}	5.02×10^{-3}	1.12×10^{-3}	4.89×10^{-3}	8.93×10^{-4}	1.48×10^{-1}	1.10×10^{-2}	5.21×10^{-3}	1.30×10^{-3}
Land use	0.0435	28.5368	0.3170	974.6366	0.0543	27.9031	0.0543	28.5476	0.3278	974.6474	0.0651	27.9139
Global Warming, Freshwater ecosystems	2.56×10^{-5}	2.25×10^{-5}	1.44×10^{-4}	4.06×10^{-5}	3.69×10^{-5}	3.39×10^{-5}	3.32×10^{-5}	3.02×10^{-5}	1.52×10^{-4}	4.82×10^{-5}	4.45×10^{-5}	4.16×10^{-5}
Freshwater eutrophication	9.07×10^{-3}	8.64×10^{-3}	3.43×10^{-2}	1.93×10^{-2}	1.75×10^{-2}	$1.71 \times 10^{-2} \times 10^{-2}$	1.28×10^{-2}	1.24×10^{-2}	3.80×10^{-2}	2.31×10^{-2}	2.12×10^{-2}	2.08×10^{-2}
Freshwater ecotoxicity	6.78×10^{-4}	4.20×10^{-4}	1.00×10^{-2}	1.23×10^{-3}	1.01×10^{-3}	7.54×10^{-4}	8.43×10^{-4}	5.85×10^{-4}	1.02×10^{-2}	1.39×10^{-3}	1.17×10^{-3}	9.19×10^{-4}
Water consumption, Aquatic ecosystems	4.77×10^{-6}	4.60×10^{-6}	1.27×10^{-5}	6.73×10^{-6}	4.85×10^{-6}	4.67×10^{-6}	9.24×10^{-6}	9.07×10^{-6}	1.72×10^{-5}	1.12×10^{-5}	9.31×10^{-6}	9.14×10^{-6}
Marine ecotoxicity	0.7912	0.6257	7.2239	1.5643	1.3151	1.1533	1.0433	0.8777	7.4760	1.8163	1.5671	1.4053
Marine eutrophication	1.10×10^{-5}	1.13×10^{-5}	2.20×10^{-5}	3.23×10^{-5}	1.23×10^{-5}	1.26×10^{-5}	2.09×10^{-5}	2.12×10^{-5}	3.19×10^{-5}	4.22×10^{-5}	2.22×10^{-5}	2.25×10^{-5}
Mineral resource scarcity	4.23×10^{-4}	7.07×10^{-5}	1.31×10^{-2}	1.06×10^{-3}	4.39×10^{-4}	9.48×10^{-5}	4.39×10^{-4}	8.64×10^{-5}	1.31×10^{-2}	1.07×10^{-3}	4.55×10^{-4}	1.10×10^{-4}
Fossil resource scarcity	2.78×10^{-2}	1.68×10^{-2}	4.22×10^{-1}	4.38×10^{-2}	4.10×10^{-2}	3.02×10^{-2}	3.46×10^{-2}	2.35×10^{-2}	4.28×10^{-1}	5.06×10^{-2}	4.77×10^{-2}	3.69×10^{-2}
TOTAL	23.6960	48.3245	177.2641	1019.427	38.5413	62.6127	31.3494	55.9779	184.9175	1027.081	46.1946	70.2661

* Output Material; OP—Open Pond; PB—Photobioreactor; FL—Flocculation; CN—Centrifugation; FN—Filtration; SO—Solvent; MI—Microwave.

Table A8. Model indices.

Indices	Description
i	Index of cultivation process alternatives (1 ... I)
j	Index of harvesting process alternatives (1 ... J)
k	Index of extraction process alternatives (1 ... K)
r	Index of recovery processes (1 ... R)
u	Index of single process units (1 ... U)
m	Index of recoverable material inputs (1 ... M)
p	Index of final products (1 ... P)
t	Index of time periods (1 ... T)

Table A9. Model parameters.

Parameter	Description
D_{pt}	Demand of final product p for period t
SP_{pt}	Selling price of final product p for period t
FC_i	Fixed cost of cultivation process alternative i
FH_j	Fixed cost of harvesting process alternative j
FE_k	Fixed cost of extraction process alternative k
FR_r	Fixed cost of recovery process r
FP_u	Fixed cost of single process unit u
OC_{it}	Operating cost of cultivation process alternative i for period t
OH_{jt}	Operating cost of harvesting process alternative j for period t
OE_{kt}	Operating cost of extraction process alternative k for period t
OR_{rt}	Operating cost of recovery process r for period t
OP_{ut}	Operating cost of single process unit u for period t
MC_{mt}	Purchase cost of material input m for period t
MK_{mt}	Purchase capacity of material input m for period t
IC_{mt}	Inventory cost of material input m for period t
IK_{mt}	Inventory capacity of material input m for period t
CC_i	Output capacity of cultivation process alternative i
CH_j	Output capacity of harvesting process alternative j
CE_k	Output capacity of extraction process alternative k
CR_r	Output capacity of recovery process r
CP_u	Output capacity of single process unit u
YC_i	Output yield of cultivation process alternative i per input material
YH_j	Output yield of harvesting process alternative j per input material
YE_k	Output yield of extraction process alternative k per input material
YR_r	Output yield of recovery process r per input material
YP_u	Output yield of single process unit u per input material
EC_i	Environmental impact per output of cultivation process alternative i
EH_j	Environmental impact per output of harvesting process alternative j
EE_k	Environmental impact per output of extraction process alternative k
ER_r	Environmental impact per output of recovery process r
EP_u	Environmental impact per output of single process unit u

Table A10. Model variables.

Variables	Description
BC_i	Binary variable, 1 if cultivation process alternative i is used
BH_j	Binary variable, 1 if harvesting process alternative j is used
BE_k	Binary variable, 1 if extraction process alternative k is used
BR_r	Binary variable, 1 if recovery process r is used
BP_u	Binary variable, 1 if single process unit u is used
PC_{it}	Production output of cultivation process alternative i for period t
PH_{jt}	Production output of harvesting process alternative j for period t
PE_{kt}	Production output of extraction process alternative k for period t
PR_{rt}	Production output of recovery process r for period t
PP_{ut}	Production output of single process unit u for period t
MQ_m	Purchase quantity of material input m for period t
BI_{mt}	Beginning inventory of material input m for period t
EI_{mt}	Ending inventory of material input m for period t
TO_{pt}	Total output of final product p for period t

References

1. International Energy Agency. Available online: www.iea:reports/world-energy-outlook-2019 (accessed on 2 March 2020).
2. Morales, M.; Collet, P.; Lardon, L.; Hélias, A.; Steyer, J.; Bernard, O. Life-cycle assessment of microalgal-based biofuel. *Biomass Biofuels Biochem.* **2019**, 507–550. [CrossRef]
3. Khan, S.; Siddique, R.; Sajjad, W.; Nabi, G.; Hayat, K.M.; Duan, P.; Yao, L. Biodiesel production from algae to overcome the energy Crisis. *Hayati J. Biosci.* **2017**, *24*, 163–167. [CrossRef]
4. Markou, G.; Vandamme, D.; Muylaert, K. Microalgal and cyanobacterial cultivation: The supply of nutrients. *Water Res.* **2014**, *65*, 186–202. [CrossRef]
5. Karamerou, E.E.; Webb, C. Cultivation modes for microbial oil production using oleaginous yeasts—A review. *Biochem. Eng.* **2019**, *151*. [CrossRef]
6. Brennan, L.; Owende, P. Biofuels from microalgae—a review of technologies for production, processing, and extractions of biofuels and co-products. *Renew. Sustain. Energy Rev.* **2010**, *14*, 557–577. [CrossRef]
7. Cheirsilp, B.; Srinuanpan, S.; Mandik, Y.I. Chapter 6—Efficient harvesting of microalgal biomass and direct conversion of microalgal lipids into biodiesel. In *Microalgae Cultivation for Biofuels Production*; Yousuf, A., Ed.; Academic Press: Cambridge, MA, USA, 2020; pp. 83–96.
8. Chisti, Y. Biodiesel from microalgae. *Biotechnol. Adv.* **2007**, *25*, 294–306. [CrossRef]
9. De Assis, T.C.; Calijuri, M.L.; Assemany, P.P.; Pereira, A.S.A.D.P.; Martins, M.A. Using atmospheric emissions as CO_2 source in the cultivation of microalgae: Productivity and economic viability. *J. Clean. Prod.* **2019**, *215*, 1160–1169. [CrossRef]
10. Culaba, A.B.; Ching, P.L.; San Juan, J.L.; Mayol, A.P.; Sybingco, E.; Ubando, A.T. A dynamic sustainability assessment of algal biorefineries for Biofuel production. In Proceedings of the 2019 IEEE 11th International Conference on Humanoid, Nanotechnology, Information Technology, Communication and Control, Environment, and Management (HNICEM), Laoag, Philippines, 29 November–1 December 2019. [CrossRef]
11. Mitra, M.; Mishra, S. Multiproduct biorefinery from *Arthrospira* spp. towards zero waste: Current status and future trends. *Bioresour. Technol.* **2019**, *291*. [CrossRef] [PubMed]
12. Mohan, S.; Hemalatha, M.; Chakraborty, D.; Chatterjee, S.; Ranadheer, P.; Kona, R. Algal biorefinery models with self-sustainable closed loop approach: Trends and prospective for blue-bioeconomy. *Bioresour. Technol.* **2019**. [CrossRef]
13. De Bhowmick, G.; Sarmah, A.K.; Sen, R. Zero-waste algal biorefinery for bioenergy and biochar: A green leap towards achieving energy and environmental sustainability. *Sci. Total Environ.* **2019**, *650*. [CrossRef]
14. Hemalatha, M.; Sravan, J.; Min, B.; Mohan, S. Microalgae-biorefinery with cascading resource recovery design associated to dairy wastewater treatment. *Bioresour. Technol.* **2019**, *284*, 424–429. [CrossRef]
15. Wu, W.; Chang, J. Integrated algal biorefineries from process systems engineering aspects: A review. *Bioresour. Technol.* **2019**, *291*. [CrossRef]
16. Sy, C.L.; Ubando, A.T.; Aviso, K.B.; Tan, R.R. Multi-objective target oriented robust optimization for the design of an integrated biorefinery. *J. Clean. Prod.* **2018**, *170*, 496–509. [CrossRef]
17. Culaba, A.B.; San Juan, J.L.; Ching, P.L.; Mayol, A.P.; Sybingco, E.; Ubando, A.T. Optimal synthesis of algal biorefineries for Biofuel production based on techno-economic and environmental efficiency. In Proceedings of the 2019 IEEE 11th International Conference on Humanoid, Nanotechnology, Information Technology, Communication and Control, Environment, and Management (HNICEM), Laoag, Philippines, 29 November–1 December 2019. [CrossRef]
18. García Prieto, C.V.; Ramos, F.D.; Estrada, V.; Villar, M.A.; Diaz, M.S. Optimization of an integrated algae-based biorefinery for the production of biodiesel, astaxanthin and PHB. *Energy* **2017**, *139*, 1159–1172. [CrossRef]

19. Gong, J.; You, F. Optimal design and synthesis of algal Biorefinery processes for biological carbon sequestration and utilization with zero direct greenhouse gas emissions: MINLP model and global optimization algorithm. *Ind. Eng. Chem. Res.* **2014**, *53*, 1563–1579. [CrossRef]
20. Ching, P.M.; Mayol, A.P.; San Juan, J.L.; Calapatia, A.M.; So, R.H.; Sy, C.L.; Ubando, A.T.; Culaba, A.B. AI methods for modeling the vacuum drying characteristics of Chlorococcum infusionum for algal Biofuel production. *Process Integr. Optim. Sustain.* **2021**. [CrossRef]
21. San Juan, J.L.; Mayol, A.P.; Sybingco, E.; Ubando, A.T.; Culaba, A.B.; Chen, W.H.; Chang, J.S. A scheduling and planning algorithm for microalgal cultivation and harvesting for biofuel production. *IOP Conf. Ser. Earth Environ. Sci.* **2020**, *463*. [CrossRef]
22. Galanopoulos, C.; Kenkel, P.; Zondervan, E. Superstructure optimization of an integrated algae biorefinery. *Comput. Chem. Eng.* **2019**, *130*. [CrossRef]
23. Caligan, C.J.; Garcia, M.M.; Mitra, J.L.; Mayol, A.P.; San Juan, J.L.; Culaba, A.B. Multi-objective optimization of water exchanges between a wastewater treatment facility and algal biofuel production plant. *IOP Conf. Ser. Earth Environ. Sci.* **2020**, *463*. [CrossRef]
24. San Juan, J.L.; Caligan, C.J.; Garcia, M.M.; Mitra, J.L.; Mayol, A.P.; Sy, C.L.; Ubando, A.T.; Culaba, A.B. Multi-objective optimization of an integrated algal and sludge-based Bioenergy Park and wastewater treatment system. *Sustainability* **2020**, *12*, 7793. [CrossRef]
25. Čuček, L.; Martín, M.; Grossman, I.E.; Kravanja, Z. Multi-period synthesis of optimally integrated biomass and bioenergy supply network. *Comput. Chem. Eng.* **2014**, *66*, 57–70. [CrossRef]
26. Chowdhury, R.; Sadhukhan, J.; Traverso, M.; Keen, P.L. Effects of residence time on life cycle assessment of bioenergy production from dairy manure. *Bioresour. Technol. Rep.* **2018**, *4*, 57–65. [CrossRef]
27. Barlow, J.; Sims, R.C.; Quinn, J.C. Techno-economic and life-cycle assessment of an attached growth algal biorefinery. *Bioresour. Technol.* **2016**, *220*, 360–368. [CrossRef]
28. Wu, W.; Lin, K.; Chang, J. Economic and life-cycle greenhouse gas optimization of microalgae-tobiofuels chains. *Bioresour. Technol.* **2018**, *267*, 550–559. [CrossRef] [PubMed]
29. Bussa, M.; Eisen, A.; Zollfrank, C.; Röder, H. Life cycle assessment of microalgae products: State of the art and their potential for the production of polylactid acid. *J. Clean. Prod.* **2018**, *213*, 1299–1312. [CrossRef]
30. Giwa, A.; Adeyemi, I.; Dindi, A.; García-Bañoz Lopez, C.; Lopresto, C.; Curcio, S.; Chakraborty, S. Techno-economic assessment of the sustainability of an integrated biorefinery from microalgae and Jatropha: A review and case study. *Renew. Sustain. Energy Rev.* **2018**, *88*, 239–257. [CrossRef]
31. Gifuni, I.; Pollio, A.; Safi, C.; Marzocchella, A.; Olivieri, G. Current Bottlenecks and Challenges of the Microalgal Biorefinery. *Trends Biotechnol.* **2019**, *37*, 242–252. [CrossRef] [PubMed]
32. Branyikova, I.; Prochazkova, G.; Potocar, T.; Jezkova, Z.; Branyik, T. Harvesting of Microalgae by Flocculation. *Fermentation* **2018**, *4*, 93. [CrossRef]
33. Su, Y.; Song, K.; Zhang, P.; Su, Y.; Cheng, J.; Chen, X. Progress of microalgae biofuel's commercialization. *Renew. Sustain. Energy Rev.* **2017**, *74*, 402–411. [CrossRef]
34. Yew, G.Y.; Lee, S.Y.; Show, P.L.; Tao, Y.; Law, C.L.; Nguyen, T.T.C.; Chang, J. Recent advances in algae biodiesel production: From upstream cultivation to downstream processing. *Bioresour. Technol. Rep.* **2019**, *7*. [CrossRef]
35. Dasan, Y.K.; Lam, M.K.; Yusup, S.; Lim, J.W.; Lee, K.T. Life cycle evaluation of microalgae biofuels production: Effect of cultivation system on energy, carbon emission and cost balance analysis. *Sci. Total Environ.* **2019**, *688*, 112–128. [CrossRef] [PubMed]
36. Biller, P.; Friedman, C.; Ross, A.B. Hydrothermal microwave processing of microalgae as a pre-treatment and extraction technique for bio-fuels and bio-products. *Bioresour. Technol.* **2013**, *136*, 188–195. [CrossRef] [PubMed]
37. Gnansounou, E.; Raman, J.K. Chapter 7—Life Cycle Assessment of Algal Biorefinery. In *Life-Cycle Assessment of Biorefineries*; Elsevier: Amsterdam, The Netherlands, 2017; pp. 199–219.
38. Solis, C.A.; Mayol, A.P.; San Juan, J.G.; Ubando, A.T.; Culaba, A.B. Multi-objective optimal synthesis of algal biorefineries toward a sustainable circular bioeconomy. *IOP Conf. Ser. Earth Environ. Sci.* **2020**, *463*. [CrossRef]